Taylor & Francis
Taylor & Francis Group

# Mechanical behaviour of phenolic coated Finnish birch plywood with simulated service damage

Joel Galos, Michael Sutcliffe & Golam Newaz

View supplementary material

Published online: 11 Aug 2016.

Submit your article to this journal

Article views: 120

View related articles

View Crossmark data

Taylor & Francis
Taylor & Francis Group

# Mechanical behaviour of phenolic coated Finnish birch plywood with simulated service damage

Joel Galos[a], Michael Sutcliffe[a] and Golam Newaz[b]

aDepartment of Engineering, University of Cambridge, Cambridge, UK; bDepartment of Mechanical Engineering, Wayne State University, Detroit, MI, USA

## ABSTRACT

This paper investigates the mechanical behaviour of Finnish birch (*Betula pendula* and *Betula pubescens*) plywood commonly used in road freight trailer decking. A series of tests have been performed to characterize the mechanical performance of the material and the effect of in-service damage that is likely to occur when the material is used in this application. Moisture damage, indentation damage, and abrasive wear are all recreated in the laboratory and the severity of each is assessed. In particular, the effect of indentation damage on flexural properties is compared against the effect of moisture damage. It is found that while indentation damage can often appear more severe during a visual inspection, it generally has a lesser effect on flexural stiffness and strength compared to moisture damage. While the effect of moisture damage on flexural properties is well documented, the effect of indentation damage is previously less well understood. Both indentation damage and moisture damage significantly increase variance in flexural stiffness, but not flexural strength. This work provides a practical insight into whether damaged road freight trailer decking can still withstand in-service loadings. It also provides a benchmark for the performance of novel deck systems such as composite sandwich panels and glass-fibre pultrusions.

## 1. Introduction

Hardwood of various varieties has been the mainstay of road freight trailer decking for decades. Indeed, there is research that suggests it is the most sustainable kind of trailer deck material, as it is renewable, recyclable, and creates lower carbon emissions in manufacture compared to steel, aluminium, and plastics (Lu *et al.* 2009). Because of the different availabilities of hardwood varieties throughout the world, the wood used in road freight trailer decking varies depending on geographic location. In Europe and the United Kingdom (UK), the most common form of hardwood used in trailer decking is Finnish birch plywood, originating in North and North Eastern Europe. The raw material of this birch plywood is composed of both *Betula pendula* and *Betula pubescens*. In North America on the other hand, oak wood decking is more common in road freight trailers.

The experience of UK road freight trailer operators indicates that water damage and indentation damage are the two most prevalent forms of in-service damage caused to hardwood trailer decking. Wear from repeated loading and unloading of grocery cages is also of concern to operators. Damaged decks are often repaired or replaced depending on the severity of damage, typically assessed through a visual inspection. There is minimal published literature that attempts to characterize the effects of these common types of in-service damage to Finnish birch plywood, and trailer operators are typically reliant on manufacturer guidelines. A

better understanding of the effects of in-service damage is crucial in helping to understand if damaged decking should be replaced. A full mechanical characterization of Finnish birch plywood trailer decking will also create a useful benchmark against which to compare new trailer decking systems.

The mechanical characterization of wood-based flooring is a relatively mature subject. The Forests Products Laboratory in the United States has developed a number of accelerated test procedures designed to characterize the performance of wood floorings (Lewis 1971). These test procedures have since been published by the American Society of the International Association for Testing and Materials (ASTM) and can be found in ASTM D 2394-05: "Standard methods for simulated service testing of wood and wood-base finish flooring" (ASTM International 2011). Within the standard, there are test procedures for measuring resistance to concentrated loading, floor surface indentation from small area loads, and damage from rolling loads. Methods for measuring the abrasion resistance, coefficient of friction, and the effects of surface wetting are also outlined in this standard.

The mechanical performance of hardwood, including Finnish birch and Finnish birch plywood, has been thoroughly addressed in literature (see Luostarinen and Verkasalo 2000). Heräjärvi (2004a) has investigated the modulus of elasticity and the modulus of rupture of Finnish birch and the relationship of these flexural properties to specific gravity. There are also industry handbooks which quantify how flexural

properties of Finnish birch plywood are affected by moisture damage (UPM 2007). Swaczyna *et al.* (2011) tested the Brinell hardness and abrasive wear resistance of eight wood species commonly used in flooring panels and found that hardness is closely related to wood density, while wear resistance has a high variance. Karshenas and Feely (1996) investigated the flexural properties and interlaminar shear strength of used plywood that had been re-used in concrete slab formwork. The experimental data were used to correlate the bending strength and bending stiffness of the used plywood. Knapic *et al.* (2012) investigated the performance of cork oak wood as a solid wood flooring. Dimensional stability to air humidity, liquid water, hardness, and wear resistance were all investigated.

The published literature and the recommendations made in ASTM D 2394-05 both give a good insight into the tests that can be used to characterize in-service damage to wood-based flooring. However, a detailed investigation into the damage types most common to hardwood road freight trailer decking will be beneficial in properly characterizing trailer deck performance. The experience of industrial partners operating large fleets of road freight trailer indicates that water damage, indentation damage and abrasive wear need to be thoroughly examined.

The aim of this paper is to determine the effect of the most common forms of in-service damage on the flexural properties of Finnish birch plywood used in road freight trailers. A particular focus of this study is to quantify the effect of indentation damage on flexural properties and to compare this to the effect of moisture damage, which is already well understood in the literature. This will provide a deeper insight into whether damaged trailer decking can still be considered fit for service, as well as provide a benchmark for the performance of novel deck systems such as composite sandwich panels and glass-fibre pultrusions. Novel deck systems are likely to be a growing area of interest as road freight fleet operators look to reduce both operation costs and carbon footprint by applying lightweight materials, among other measures, in trailer design (Galos *et al.* 2015).

## 2. Materials and methods

### 2.1. Materials

Finnish birch (*B. pendula* and *B. pubescens*) plywood, trade name WISA-Trans, manufactured by UPM-Kymmene Corporation is the focus of this investigation. This plywood is the most common material used in road freight trailer decking in Europe and the UK. It is also used extensively in other industries, such as in formwork panels in the construction industry. Stewart (2005) provides a description of the process used to fabricate these specific plywood panels. Of particular importance to the application is the phenolic coating that is applied to the exposed surfaces and exposed edges of the laminate in order to improve wear performance and minimize moisture uptake during service life. The top surface is hot-pressed with a non-slip pattern to give the finished plywood laminate.

**Table 1.** Stiffness and strength properties of pristine WISA-Trans birch plywood subjected to a wheel loading over a contact area of $180 \times 80$ mm in accordance with ISO 1496 (note: no load factor applied) (UPM 2014).

| Thickness (mm) | Span = 400 mm | | Span = 500 mm | |
|---|---|---|---|---|
| | $P_{max}$ (kg) | $\delta_{max}$ (mm) | $P_{max}$ (kg) | $\delta_{max}$ (mm) |
| 27 | 2800 | 8.4 | 2400 | 11.1 |
| 28 | 3000 | 7.7 | 2700 | 10.7 |
| 30 | 3300 | 7.5 | 2900 | 10.1 |

Note: $P_{max}$ = ultimate wheel load and $\delta_{max}$ = deflection at $P_{max}$.

Samples were cut from 30 mm nominal thickness (21 ply) panels for each of the test types and all tests were performed at room temperature. Typically five samples were tested in each of the different tests described below. Cutting the samples from a larger plywood panel resulted in the edges of the specimens being exposed with no phenolic coating. In practice, the edges will always be coated with phenolic adhesive to minimize the moisture uptake of the wood.

The plywood has two principal material directions which correspond to the orientation of the outer veneers, indicated by the direction of an arrow (printed on by the manufacturer) on the back face of the material. Parallel to the direction of the arrow is defined here to be the 0° direction and perpendicular to the arrow is defined to be the 90° direction. Because of its directionality, Finnish birch plywood is generally laid over trailer chassis beams so that the 0° orientation is in three-point bending, as this direction is considerably stiffer and stronger than the 90° direction.

WISA-Trans decking is designed to conform to ISO 1496: "The specification and testing of general cargo containers for general purposes" (ISO 1990). The manufacturer provides data (Table 1) on the maximum load $P_{max}$ and corresponding maximum deflection $\delta_{max}$ resulting from the wheel load of a forklift, as recommended by the standard. Data for the most common thicknesses and span lengths used in road freight trailer decking are provided in Table 1.

### 2.2. Flexural testing

Three-point bending tests are performed at room temperature to determine the flexural stiffness and strength of both pristine and damaged specimens. In all scenarios, at least five specimens are tested and results averaged. Pristine specimens are tested in both the 0° and 90° orientations described above, while the damaged specimens are only tested in the 0° orientation as this is the typical in-service load orientation. The reproduction of moisture damage and indentation damage in flexural test specimens is explained in more detail in the following two sections.

The three-point bending method is chosen since this is the loading configuration commonly applied in-service from forklift and grocery cage wheels. However, it has been observed that 10–15% lower values for flexural properties have been found using the three-point bending method compared to the four-point bending method for wood products, including cross-grain laminates of plywood (Bodig and Jayne 1982). In spite of this, the flexural properties obtained from this testing regime are used to compare the effects of different types of damage, and for this purpose, the three-point method is appropriate.
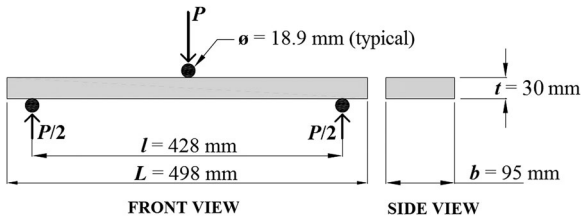
**Figure 1.** Specimen dimensions and test parameters used in three-point bend testing.

The three-point bend test set-up and specimen parameters are shown in Figure 1. A span to thickness ratio of approximately 15/1 is used to ensure that the specimens will fail in bending. The span length of 428 mm used in testing was the maximum allowable span length given the fixture and test machine used. This is close to the 450 mm span length that is typically used in a standard 13.6 m UK road freight trailer. All three-point bend tests are performed on an Instron tensile test machine using a test speed of 5 mm/min and a laser displacement sensor is used to capture displacement at the mid-span.

The ultimate flexural stress $\sigma_{ult}$ is calculated using the maximum load $P_{max}$ observed at failure, the unsupported span length $l$, the specimen width $b$, and the specimen thickness $t$:

$$\sigma_{ult} = \frac{3lP_{max}}{2bt}. \tag{1}$$

The flexural modulus $E$ is calculated using the gradient $k$ of the initial linear portion of the load deflection curve obtained during testing:

$$E = \frac{l^3 k}{4bt^3}. \tag{2}$$

### 2.3. Moisture damage

Specimens for flexural testing are subjected to varying levels of moisture damage through immersion in a water tank at room temperature, over six differing time intervals as defined in Table 2. At each time interval examined, five specimens are removed from the water tank and excess water is towel dried from the surface of the specimens. The moisture content of each specimen is then determined by the percentage of weight gained (averaged results for each time interval shown in Table 2). The specimens are subjected to the flexural testing regime described in Section 2.2 and results from the five specimens are averaged.

**Table 2.** Average moisture content by weight (with standard deviations) of pristine 21-ply phenolic coated Finnish birch plywood, over six different time intervals.

| Duration of soaking (hours) | Moisture content by weight (%) |
| --- | --- |
| 1.3 | 6.2 ± 0.8 |
| 22 | 16 ± 1.3 |
| 48 | 19 ± 1.4 |
| 331 | 31 ± 1.8 |
| 616 | 44 ± 1.3 |
| 834 | 44 ± 0.8 |

The soaking of specimens within the water tank represents an extreme case of moisture damage that is very unlikely to occur in-service, but is used to produce accelerated moisture damage. However, this approach allows for an analytical model of diffusivity to be applied with more confidence via the use of Fickian diffusion theory as outlined by Crank (1975). This assertion is supported by the fact that moisture has a tendency to travel parallel to the grain through vessels in individual veneers, as observed when food red dye is left soaking within a hole drilled halfway through the thickness (Figure 2). The diffusivity of the adhesive bond line between veneers will also have an influence on the distribution of moisture (Gereke and Niemz 2010), however, this effect is neglected to simplify the analysis.

By assuming that the specimens can be approximated by a one-dimensional infinite plate, the moisture concentration $C$ with respect to time $T$ in a plate with a thickness co-ordinate $x$ can be described by Fickian theory for steady-state diffusion in Equations (3)–(5) (Vinson 1977),

$$\frac{\partial C}{\partial T} = D_x \frac{\partial^2 C}{\partial x^2}, \tag{3}$$

$$C(x, 0) = C_i, \tag{4}$$

$$C(0, T) = C(t, T) = C_a, \tag{5}$$

where $C_a$ is ambient moisture concentration, $C_i$ is initial moisture concentration in the material, and $D_x$ is diffusivity through the thickness. The solution to Equations (3)–(5) at plate thickness $t$ is given by Equation (6), adapted from Vinson (1977).

$$\frac{C - C_i}{C_a - C_i} = 1 - \frac{4}{\pi} \sum_{n=0}^{\infty} \frac{1}{(2n + 1)} \sin\left[\frac{(2n + 1)}{t}\right]$$

$$\times \exp\left[\frac{-(2n + 1)^2 \pi^2 D_x T}{t^2}\right]. \tag{6}$$

The total weight gain $m$ from moisture absorption is then determined by integrating the moisture concentration over the plate thickness (Equation (7)) which yields Equation (8),

$$m = \int_0^t C \, dx, \tag{7}$$

$$G = \frac{m - m_i}{m_\infty - m_i} = 1 - \frac{8}{\pi^2} \sum_{n=1}^{\infty} \frac{\exp\left[-(2n + 1)\pi^2 \left(\frac{D_x T}{t^2}\right)\right]}{(2n + 1)^2}, \tag{8}$$

where $m_\infty$ is the moisture weight gain in the material when equilibrium has been reached with the ambient humidity. Assuming an initial dry state, the moisture weight gain can be described as a percentage $M$ (Equation (9)), which is a product of $G$ (Equation (8)) and the percentage weight gain in the material when in equilibrium with its environment $M_\infty$. Equation (8) has been shown to have an approximate numerical solution of Equation (10) (Vinson 1977).

$$M = GM_\infty, \tag{9}$$

$$G = 1 - \exp\left[-7.3\left(\frac{D_x T}{t^2}\right)^{0.75}\right]. \tag{10}$$

**Figure 2.** Diffusion of red dye outward from a central hole indicates that moisture has a tendency to travel parallel to the grain through vessels in individual veneers.

For small values of $t$, Equation (10) can be expressed as:

$$G = 4\sqrt{\frac{D_x T}{\pi t^2}}. \qquad (11)$$

Using Equation (8), through thickness diffusivity $D_x$ can then be expressed as Equation (12). Through thickness diffusivity can also be determined from the initial slope of the curve of the moisture gain as a function of square root of time.

$$D_x = \frac{\pi}{16} t^2 \left[\frac{m}{m_\infty \sqrt{T}}\right]^2. \qquad (12)$$

## 2.4. Indentation damage

Indented birch plywood specimens for flexural testing are prepared at room temperature with either three or six indentations across the width at the centre of each specimen as shown in Figure 3. These specimens are of the same dimensions as those shown in Figure 1. Indentations are created with a 25.5 mm diameter hardened steel spherical indenter with an applied load of 10 kN. Multiple indentations across the central width represent the most severe form of indentation damage likely to occur during the service lifetime of trailer decking. This damage is analogous to a forklift driving over foreign object debris on the surface of the trailer decking, which is a relatively common occurrence in everyday road freight operations.

When Finnish birch plywood is permanently indented, a load cycle plot like that shown in Figure 4 can be created. This plot reflects the interaction between the test specimen material properties (Young's modulus, Poisson's ratio, initial flow stress, and strain hardening) and the elastic material properties of the indenter (Young's modulus and Poisson's ratio). The shape of the load cycle curve here indicates that elastic/plastic indentation takes place, whereby the material is indented to a total depth of $\delta_{total}$ at a maximum indenting force of $F_{max}$, before relaxing during unloading to leave a residual dent of depth $\delta_{residual}$. The area within the hysteresis loop of the load cycle plot represents the plastic work of indentation and is a useful quantity in characterizing indentation damage. This type of indentation has been successfully modelled and is well understood in literature (Field and Swain 1993, Weppelmann et al. 1993).

In addition to the specimens described above that were indented and subsequently tested in three-point bending, other pristine full thickness birch plywood specimens were only tested by indentation at room temperature. In particular, hardened steel spherical indenters of diameter 25.5 mm and 40.0 mm, as well as a nylon castor wheel (typical of that used in the road freight industry) of diameter 125 mm, have all been investigated. A loading rate of 2.0 mm/min is used in all cases and specimens are loaded from 2 to 12 kN at increments of 2 kN. The samples are supported from the underside to prevent the introduction of bending effects. Contact profilometry was performed using a Taylor Hobson Form Talysurf 120 to measure the residual dent depths $\delta_{residual}$. Multiple measurements are taken at each indent location to minimize the chance of missing the point of maximum dent depth. The correlations between the maximum indentation force $F_{max}$,
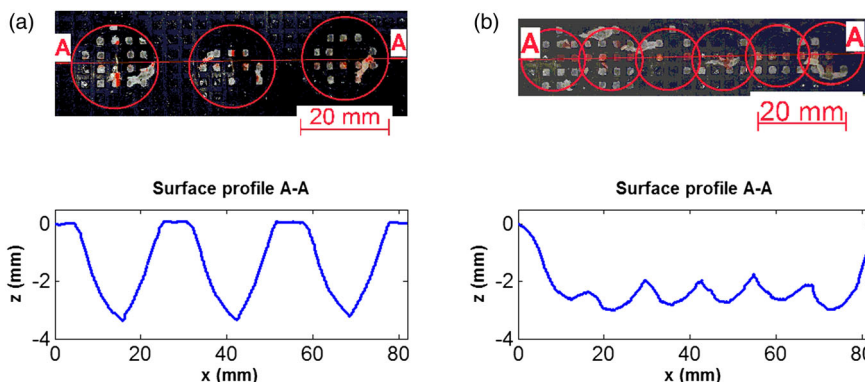


**Figure 3.** Top views and surface profiles of flexural test specimens with (a) three indentations and (b) six indentations across the centre of the specimen. Note: Indentations are created with a 25.5 mm diameter hardened steel spherical indenter at an applied load of 10 kN.
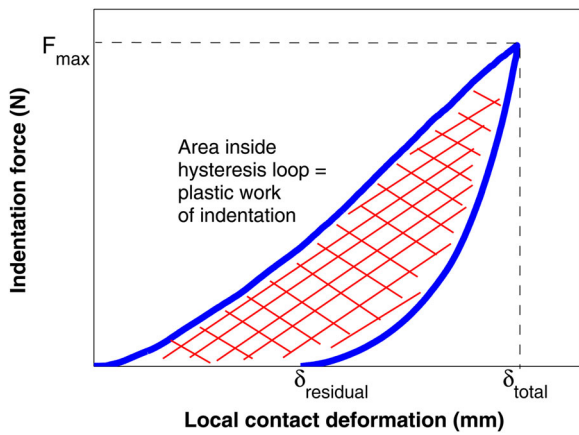
**Figure 4.** Load cycle plot of an elastic/plastic indentation, where the area inside the hysteresis loop is defined as the plastic work of indentation.
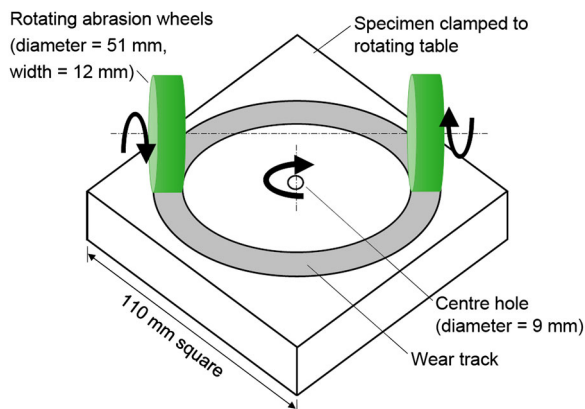
the residual dent depth $\delta_{residual}$, and the plastic work of indentation are then examined.

Brinell hardness can also be used to characterize indentation resistance and is calculated from the applied load $P$, the diameter of the indenter $D$, and the diameter of the residual indentation $d$, as shown in Equation (13).

$$BH = \frac{2P}{\pi D(D - \sqrt{D^2 - d^2})}. \quad (13)$$

### 2.5. Wear testing

Road freight trailer decking is often subjected to rolling loads from grocery cage wheels, which can cause a significant amount of wear to the exposed surface. It is therefore important to characterize the wear performance and the effect of the non-slip phenolic coating. An accelerated wear test machine is used to analyse the wear performance of both pristine phenolic coated birch plywood (WISA-Trans) and pristine birch plywood that has had the phenolic coating removed. A schematic of the test set-up used in all tests is shown in Figure 5. All tests were performed at room temperature using H18 Taber abrasion wheels that are composed of a vitrified binder and aluminium oxide abrasive particles, which deliver a medium coarse abrasive action.

The Archard wear equation (Equation (14)) defines wear rate as the volume lost from the wearing surface divided by the sliding distance. Wear rate typically depends on the normal load being applied, the relative sliding speed, the initial temperature, as well as the thermal and mechanical properties of the materials in contact (Hutchings 1992).

$$\text{Wear rate} = \frac{\text{Volume lost from wearing surface}}{\text{Sliding distance}}. \quad (14)$$

In wear testing of floor materials, the mass loss during testing is often measured and related back to the volume lost from the wearing surface by knowing the density of the material being tested. However, because the phenolic coating has a different density from wood, the average wear depth is the strongest candidate to characterize wear volume in this case. Hence, contact profilometry was performed using a Taylor Hobson Form Talysurf 120 to measure the wear depth at numerous locations of the wear track and average values are reported.
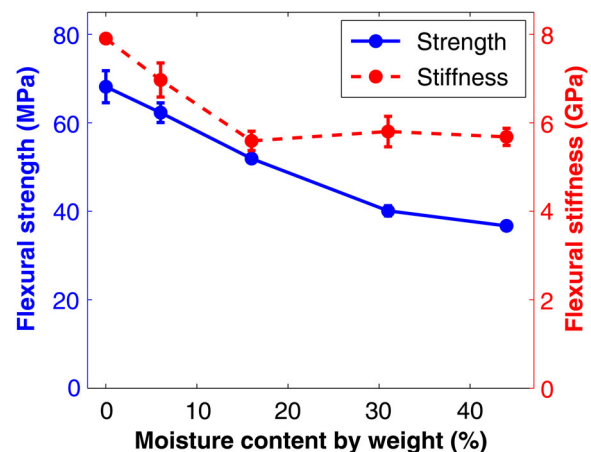
## 3. Results and discussion

### 3.1. Flexural testing

A summary of results obtained from the three-point bend tests of pristine specimens is provided in Table 3. It should be noted that the values of flexural properties may be slightly underestimated because of the three-point bending method (Bodig and Jayne 1982). For the specimens with water

**Table 3.** Summary of averaged results (with standard deviations) from three-point bend testing of pristine 21-ply Finnish birch plywood with a nominal thickness of 30 mm.

| Orientation | No. of specimens | $P_{max}$ (kN) | $\delta_{max}$ (mm) | $\sigma_{ult}$ (MPa) | $E$ (GPa) |
|---|---|---|---|---|---|
| Longitudinal (0°) | 5 | 8.8 ± 0.5 | 13 ± 1.0 | 68 ± 3.2 | 7.9 ± 0.08 |
| Transverse (90°) | 5 | 5.8 ± 0.9 | 11 ± 0.9 | 45 ± 5.0 | 5.3 ± 0.18 |



**Figure 5.** Rotary abrasion test set-up for accelerated wear testing. Note: Test speed = 72 RPM, applied load = 1 kg per wheel. Not to scale.
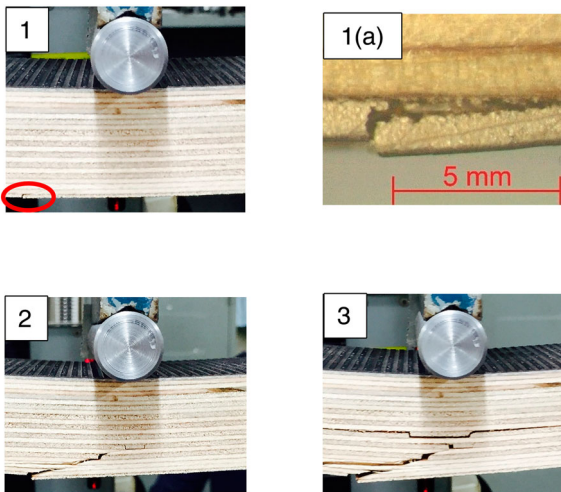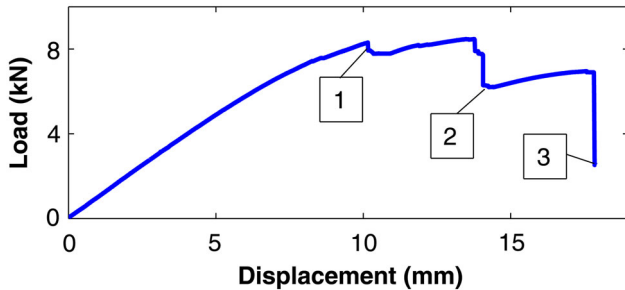


**Figure 6.** Flexural strength and stiffness (determined by three-point bend tests) of Finnish birch plywood plotted against moisture content by weight. Note: Error bars plotted correspond to standard deviation.
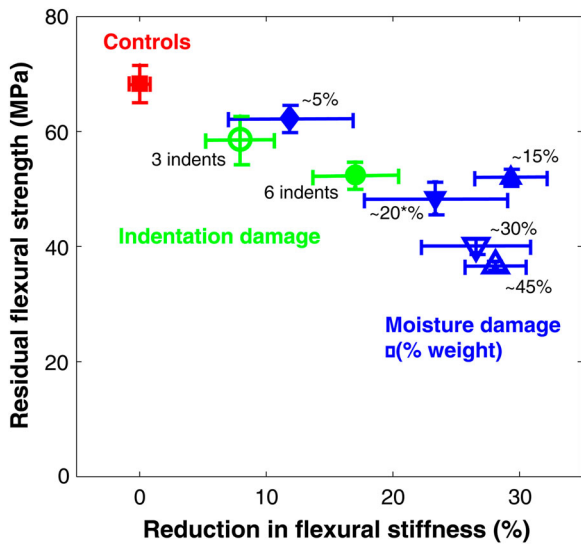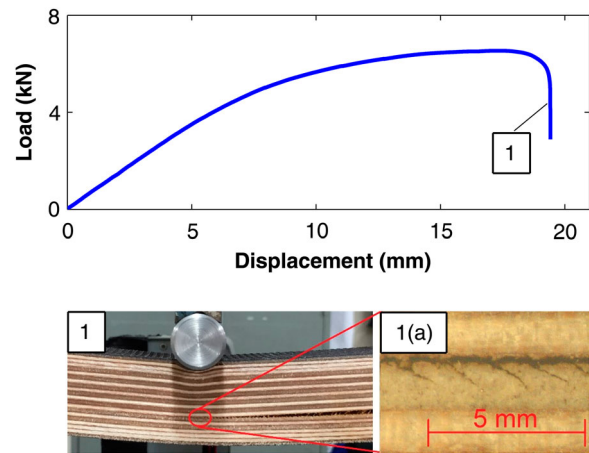
**Figure 7.** Residual flexural strength (determined through three-point bend tests) of Finnish birch plywood decking with varying levels of damage, plotted against the reduction in flexural stiffness.
Note: Error bars plotted correspond to standard deviation. *Dried from 20% to 10% moisture.



**Figure 9.** Typical load–displacement curve and corresponding failure mechanism for Finnish birch plywood (30 mm nominal thickness) with moisture damage in three-point bending.
Note: Inset photo and micrograph correspond to the position indicated on the load–displacement curve.

damage, the flexural strength and flexural stiffness are plotted against the percentage of moisture by weight in Figure 6. The residual flexural strength of specimens with indentation damage and water damage are compared in Figure 7. Both

indentation damage and water damage are characterized through the loss in flexural stiffness compared to the stiffness of pristine specimens. It is evident from Figure 7 that indentation damage can have a significant impact on the flexural properties of Finnish birch plywood. However, while indentation damage can look severe upon visual inspection, testing has shown that water damage, which can look far less severe, can have a greater effect on residual strength and stiffness. Increased levels of variance in flexural stiffness were also observed for all damaged specimens, however, the variance in flexural strength was not significantly affected by damage (Figure 7).

Representative load deflection curves with corresponding failure mechanisms for both pristine and moisture damaged specimens are shown in Figures 8 and 9, respectively. Failure in dry specimens (both pristine and indented) was generally initiated at the tension side (lower side in three-
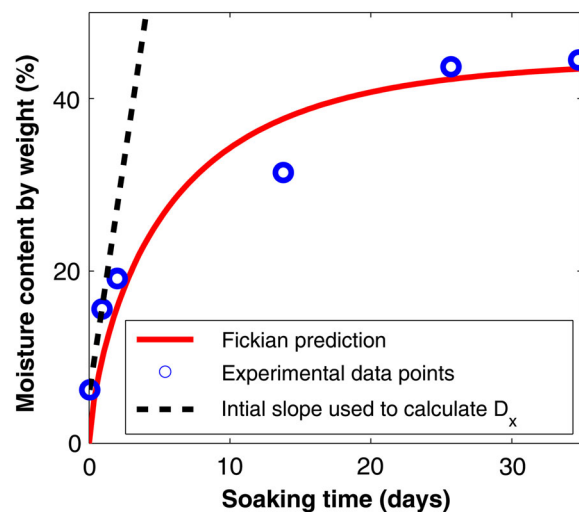


**Figure 8.** Typical load–displacement curve and corresponding failure mechanisms for pristine Finnish birch plywood (30 mm nominal thickness) in three-point bending.
Note: Inset photos correspond to the positions indicated on the load–displacement curve.



**Figure 10.** Moisture content by weight plotted against specimen soaking time. Experimental data points are a reasonable fit with Fickian diffusion theory calculated from the through thickness diffusivity $D_x$ determined from the slope given by the first two experimental data points.
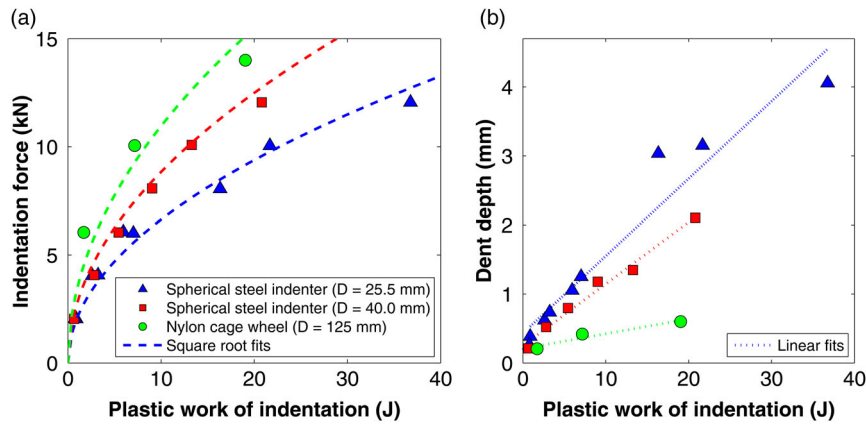
**Figure 11.** (a) Maximum indentation force and (b) residual dent depth plotted against plastic work of indentation.

point bend tests) of the specimens (Figure 8(1, 1(a))). The tensile fracture propagates through the bottom core veneers as they subsequently carry additional load (Figure 8 (2)). Finally, a delamination initiates at a central veneer and propagates along the length of the specimen (Figure 8(3)), while the top veneers remain intact carrying the residual load.

Failure in specimens with moisture damage was found to be dominated by interlaminar delamination between core veneers (Figure 9), which could be attributed to moisture accumulating between veneers (Gereke and Niemz 2010). Ruponen *et al.* (2014) suggested that this tendency of birch plywood with moisture damage to delaminate can be reduced or eliminated through binderless bonding of veneers and a post-manufacture thermal modification.

## 3.2. Moisture damage

The through thickness diffusivity $D_x$ is found to be 9.9 mm$^2$/day from the initial slope of the curve of the moisture gain as a function of square root of time (Figure 10). This has the same order of magnitude as other plywood materials (Liu and Simpson 1999, Cai 2005). It can be seen in Figure 10 that experimental data points for moisture increase with soaking time closely follow Fickian diffusion theory. It is evident from both the experimental data and analytical model that the maximum moisture content likely to be attained in Finnish birch plywood when fully immersed in water is approximately 45% by weight. The small differences between the experimental data points and the Fickian prediction are attributed to the assumptions that the diffusion is steady state and that specimens have an initial dry state, when in reality there is a small amount of moisture present at atmospheric conditions. The different moisture diffusivity of the adhesive layers may also be causing moisture to accumulate at the bond lines (Gereke and Niemz 2010).

## 3.3. Indentation damage

The maximum indentation force $F_{max}$ and residual dent depth $\delta_{residual}$ are plotted against the plastic work of indentation in Figure 11. The residual dent depth is found to vary linearly with plastic work of indentation, while the maximum

indentation force exhibits a square root correlation with the plastic work of indentation, which is to be expected for this type of quasi-static load arrangement (Sutcliffe *et al.* 2012).

The Brinell hardness was determined at various loads (8, 10, and 12 kN) with an indenter diameter of 25.5 mm and the average value is found to be 27 MPa. This is in good agreement with the Brinell hardness of Finnish birch reported by Heräjärvi (2004b), who found the Brinell hardness of *B. pendula* and *B. pubescens* to be 23.5 and 20.5 MPa, respectively. The results are also comparable to those reported for similar kinds of hardwood varieties used in flooring panels (Swaczyna *et al.* 2011).
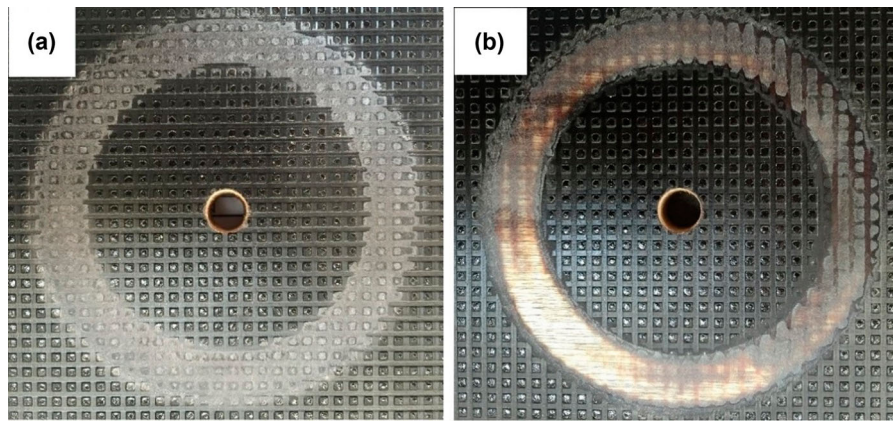
## 3.4. Wear testing

A summary of results of the accelerated wear testing of both phenolic coated and uncoated specimens is shown in Figure 12. While phenolic coating is not commonly used in other types of wood flooring, it can be seen that the presence of the phenolic coating generally greatly improves the wear resistance of the birch plywood. The wear testing results of the uncoated birch plywood specimens support the notion
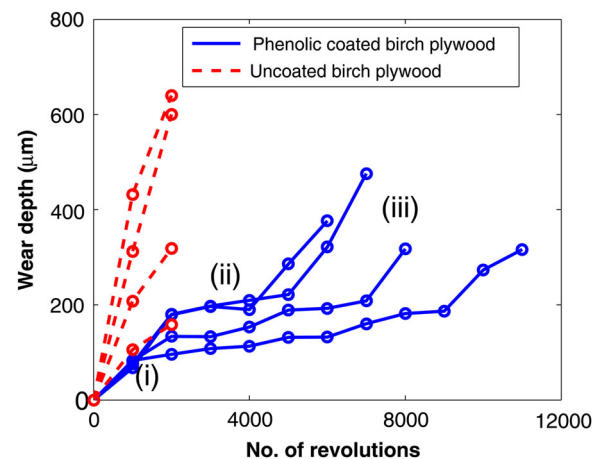


**Figure 12.** Maximum wear depth of coated and uncoated Finnish birch plywood plotted against the number of revolutions of the rotary abrasion machine for four repeated tests. Three distinct stages of wear observed in the phenolic coated specimens indicated.

**Figure 13.** Wear of phenolic coated Finnish birch plywood after testing on rotary abrasion machine for (a) 1000 revolutions as the tops of the non-slip phenolic coating are worn off and (b) 7000 revolutions as the birch plywood becomes exposed.

that a high level of variance is to be expected in the wear resistance of uncoated wood floor materials (Swaczyna *et al.* 2011).

It is evident that the phenolic coated specimens progress through three distinct stages of wear, as labelled in Figure 12:

(i) Initial period of running-in where the tips of the phenolic coating are worn off to leave a wear track surface like that shown in Figure 13(a).

(ii) Steady low-wear regime where the bulk of the phenolic coating is slowly worn down.

(iii) Final high-wear period where the phenolic coating is removed exposing the birch plywood, leaving a wear track like that shown in Figure 13(b).

## 4. Conclusions

From the mechanical testing regime used to characterize the performance of phenolic coated Finnish birch (*B. pendula* and *B. pubescens*) plywood, the following conclusions can be drawn:

- Indentation damage can have a significant impact on residual flexural properties.
- While indentation damage can look severe during a visual inspection, it generally has a lesser effect on flexural stiffness and strength compared to moisture damage. However, indentation damage does also increase the variance in flexural stiffness.
- Moisture damage considerably reduces flexural strength and stiffness, while significantly increasing variance in flexural stiffness.
- Moisture damage changes the failure mode of Finnish birch plywood in three-point bending. A tensile fracture of the bottom veneer is likely to occur in pristine and indented specimens, while delamination of central veneers becomes the typical failure mode for specimens with moisture damage.
- Fickian theory of steady-state diffusion provides a reasonable approximation of the water diffusion process in Finnish birch plywood when it is completely immersed in water.

- The hot-pressed non-slip phenolic coating typically applied to this material greatly improves the wear performance. However, significant levels of variance are observed during, accelerated wear testing.
- The testing regime here has provided useful data that helps to quantify the extent to which damaged road freight trailer decking can still withstand in-service loadings. It also provides a benchmark for the performance of novel deck systems such as composite sandwich panels and glass-fibre pultrusions.

## Disclosure statement

No potential conflict of interest was reported by the authors.

## References

ASTM International (2011) *ASTM D2394-05. Standard Methods for Simulated Service Testing of Wood and Wood-Base Finish Flooring* (Philadelphia, PA: Annual Book of ASTM Standards).

Bodig, J. and Jayne, B. A. (1982) *Mechanics of Wood and Wood Composites* (New York: Van Nostrand Reinhold).

Cai, L. (2005) Determination of diffusion coefficients for sub-alpine fir. *Wood Science and Technology*, 39 (2), 153–162.

Crank, J. (1975) *The Mathematics of Diffusion*, 2nd ed. (Oxford, UK: Clarendon Press).

Field, J. S. and Swain, M. V. (1993) A simple predictive model for spherical indentation. *Journal of Materials Research*, 8 (2), 297–306.

Galos, J., Sutcliffe, M., Cebon, D., Piecyk, M. and Greening, P. (2015) Reducing the energy consumption of heavy goods vehicles through the application of lightweight trailers: Fleet case studies. *Transportation Research Part D: Transport and Environment*, 41, 40–49.

Gereke, T. and Niemz, P. (2010) A numerical study on the influence of the bond-line diffusivity on moisture-related stresses and deformations of three-layered spruce cross-laminates. *Wood Material Science and Engineering*, 5, 62–66.

Heräjärvi, H. (2004a) Static bending properties of Finnish birch wood. *Wood Science and Technology*, 37, 523–530.

Heräjärvi, H. (2004b) Variation of basic density and Brinell hardness within mature Finnish *Betula pendula* and *B. pubescensstems*. *Wood and Fiber Science*, 36 (2), 216–227.

Hutchings, I. (1992) *Tribology: Friction and Wear of Engineering Materials* (Cambridge, UK: Edward Arnold).

ISO (1990) *ISO 1496-1: Series 1 Freight Containers – Specification and Testing – Part 1, General Cargo Containers* (Geneva, Switzerland: International Organization for Standardization).

Karshenas, S. and Feely, J. (1996) Structural properties of used plywood. *Construction and Building Materials*, 10 (8), 553–563.

Knapic, S., MacHado, J. S. and Pereira, H. (2012) Properties of cork oak wood related to solid wood flooring performance. *Construction and Building Materials*, 30, 569–573.

Lewis, W. (1971) *Simulated Service Testing of Wood and Wood-Base Finish Flooring* (Madison, WI: United States Department of Agriculture Forest Service, Forest Products Laboratory).

Liu, J. Y. and Simpson, W. T. (1999) Two-stage moisture diffusion in wood with constant transport coefficients. *Drying Technology*, 17 (1–2), 258–267.

Lu, J., Chorney, M. and Peterson, L. (2009) Sustainable trailer flooring. *BioResources*, 4 (2), 835–849.

Luostarinen, K. and Verkasalo, E. (2000) Birch as sawn timber and in mechanical further processing in Finland. A literature review. *Silva Fennica Monographs*, 1, 1–40.

Ruponen, J., Rautkari, L., Belt, T. and Hughes, M. (2014) Factors influencing properties of parallel laminated binderless bonded plywood manufactured from rotary cut birch (*Betula pendula* L.). *International Wood Products Journal*, 5 (1), 11–17.

Stewart, P. (2005) Latest innovations in formwork plywood panels. *Concrete (London)*, 39, 22–24.

Sutcliffe, M., Aceves, C. M., Stronge, W. J., Choudhry, R. S. and Scott, A. E. (2012) Moderate speed impact damage to 2D-braided glass–carbon composites. *Composite Structures*, 94 (5), 1781–1792.

Swaczyna, I., Kedzierski, A., Tomusiak, A., Cichy, A. and Rozanska, A. (2011) Hardness and wear resistance tests of the wood species most frequently used in flooring panels. *Forestry and Wood Technology*, 87 (76), 82–87.

UPM-Kymmene Corporation (2007) *Handbook of Finnish Plywood*. Finnish Forest Industries Federation (Lahti, Finland: Kirjapaino Markprint Oy).

UPM-Kymmene Corporation (2014) WISA-Trans. Product catalogue. Accessed 31 July 2014, available at: http://www.wisaplywood.com/en/downloads/brochures/transport/Documents/WISA-Trans_EN_fs.pdf

Vinson, J. R. (1977) *Advanced Composite Materials: Environmental Effects* (Philadelphia, PA: American Society for Testing and Materials).

Weppelmann, E. R., Field, J. S. and Swain, M. V. (1993) Observation, analysis, and simulation of the hysteresis of silicon using ultra-micro-indentation with spherical indenters. *Journal of Materials Research*, 8 (4), 830–840.